ORIENTAL JOURNAL OF CHEMISTRY
An International Open Access, Peer Reviewed Research Journal
www.orientjchem.org
ISSN: 0970-020 X
CODEN: OJCHEG
2026, Vol. 42, No.(3):
Pg.924-938

Formulation and in-Vitro Evaluation of Gastroretentive Floating Tablets of Axitinib: Optimization Using 3^3 Full Factorial Design of Experiments

SANGMESH MALLIKARJUN CHAUDHARI* and RAJKUMARI THAGELE[1]

*[1]Career Point School of Pharmacy, Career Point University, Kota, Rajasthan
*Corresponding author: sangmesh.chaudhari@gmail.com

http://dx.doi.org/10.13005/ojc/420313

(Received: November 13, 2025; Accepted: January 07, 2026)

ABSTRACT

Axitinib, a selective vascular endothelial growth factor receptor (VEGFR) tyrosine kinase inhibitor approved for the management of advanced renal cell carcinoma, exhibits pH-dependent solubility and a narrow absorption window predominantly confined to the gastric and proximal intestinal mucosa. Rapid gastric transit of conventional oral dosage forms limits effective drug absorption, leading to erratic plasma concentrations and suboptimal therapeutic outcomes. The present study aimed to develop and optimize a gastroretentive floating tablet system of axitinib to enhance gastric residence time, promote drug dissolution in the acidic gastric environment, and improve oral bioavailability. Floating tablets were manufactured by direct compression employing hydroxypropyl methylcellulose (HPMC K4M/K100M) as the hydrophilic matrix-forming polymer and sodium bicarbonate as the effervescent gas-generating agent. A 3^3 full factorial Design of Experiments (DoE) was applied to evaluate the independent and interactive effects of HPMC concentration (X_1: 15–25% w/w), Carbopol 934P (X_1: 2–6% w/w), and sodium bicarbonate (X_1: 5–10% w/w) on critical quality attributes including floating lag time, total floating time, drug release at 12 h, and tablet hardness. Three-dimensional response surface plots were generated for visual interpretation of factor–response relationships. Preformulation studies confirmed axitinib's physicochemical suitability and excipient compatibility. All formulations demonstrated acceptable powder flow and post-compression parameters. In-vitro buoyancy studies showed rapid floating onset (<90 s) and sustained floating for >9 h across all batches. The optimized formulation F14 exhibited a floating lag time of 44 ± 2 s, total floating duration of 13.4 ± 0.7 h, and cumulative drug release of 94.6 ± 1.5% at 12 h following Korsmeyer–Peppas and Higuchi release kinetics (n = 0.63), indicating diffusion-controlled non-Fickian transport. Gastroprotective evaluation confirmed structural integrity and pH stability over 12 h. The developed floating gastroretentive system represents a promising platform for enhancing axitinib biopharmaceutical performance.

Keywords: Axitinib; Floating gastroretentive tablets; HPMC; Sodium bicarbonate; Design of Experiments; Response surface methodology; Sustained release; Non-Fickian diffusion; Renal cell carcinoma.

INTRODUCTION

Oral drug delivery is the most widely preferred route of administration in modern pharmacotherapy owing to its non-invasive nature, patient convenience, cost-effectiveness, and flexibility in formulation design[1, 2]. However, various anatomical and physiological factors inherent to the gastrointestinal tract present significant challenges to the oral bioavailability of many therapeutically important drugs. These include variable gastric emptying rates, differences in regional pH, mucosal barriers, and short gastric residence times that are often inadequate for complete dissolution of drugs exhibiting pH-dependent solubility or narrow regional absorption[3–5].

Gastroretentive drug delivery systems (GRDDS) have emerged as a scientifically rational solution to these challenges. By prolonging the residence of a dosage form within the stomach, GRDDS ensures continued drug release at the primary absorption site, maintains drug levels within the therapeutic window, and reduces dosing frequency—an important consideration for drugs requiring long-term administration[6, 7]. Among the various GRDDS platforms, floating systems have been most extensively investigated and clinically validated. Floating tablets retain buoyancy through low bulk density, hydrophilic gel matrix formation, or gas-generation mechanisms, the last of which is commonly achieved via sodium bicarbonate that reacts with gastric acid to produce CO_1, enabling the tablet to float above the gastric contents[8, 9].

Axitinib (5-[(1E)-2-(pyridin-2-yl)vinyl]-N-(2-(trifluoromethyl)-phenyl)-1H-indazole-6-carboxamide) is a potent, selective second-generation VEGFR-1/2/3 inhibitor used as a standard-of-care agent in the treatment of advanced clear-cell renal cell carcinoma after failure of prior systemic therapy[10, 11]. The drug exhibits markedly higher aqueous solubility under acidic gastric conditions (pH 1.2) compared to neutral or basic environments, with absorption principally occurring in the stomach and upper gastrointestinal tract[12]. The Biopharmaceutics Classification System classifies axitinib as a Class II compound—low aqueous solubility at intestinal pH but high intestinal permeability—with variable oral bioavailability (~58%) governed significantly by dissolution kinetics[13, 14]. Frequent dosing (twice daily) and high interpatient pharmacokinetic variability further complicate its clinical management[15, 16].

Hydrophilic polymers such as hydroxypropyl methylcellulose (HPMC) are the cornerstone of floating matrix tablet technology. HPMC hydrates rapidly in gastric fluid to form a swellable gel matrix that entraps CO_1 generated from sodium bicarbonate, maintains tablet buoyancy, and modulates drug diffusion through the hydrated network[17, 18]. The gel layer thickness, drug diffusion coefficient, and matrix erosion rate are all influenced by the concentration and viscosity grade of HPMC used, providing a tunable sustained-release profile. Carbopol 934P contributes to additional matrix viscosity and bioadhesive character when incorporated in combination with HPMC[19, 20].

Design of Experiments (DoE) methodology represents a gold standard for systematic formulation optimization, enabling quantitative evaluation of main effects, interaction effects, and quadratic effects of selected formulation variables on key response attributes[21, 22]. Three-dimensional response surface plots generated through DoE analysis provide critical visual insight into the nature and magnitude of factor–response relationships, facilitating rational identification of optimal formulation conditions[23, 24]. A 3^3 full factorial design is particularly suitable for evaluating three independent variables at three levels each, generating 27 experimental runs that capture the full design space without assumptions of linearity[25].

Despite the recognized biopharmaceutical limitations of axitinib and the well-established utility of floating gastroretentive systems, there remains a notable paucity of systematic studies specifically addressing floating gastroretentive tablet development for this molecule. The present investigation, therefore, aims to develop, optimize using DoE, and comprehensively evaluate gastroretentive floating tablets of axitinib with the aid of three-dimensional response surface analysis.

MATERIALS AND METHODS

Materials

Axitinib was received as a gift sample and employed as the active pharmaceutical ingredient.

Hydroxypropyl methylcellulose (HPMC K4M and K100M) was used as the primary hydrophilic matrix-forming polymer to provide tablet integrity, gel formation, and sustained drug release. Sodium bicarbonate ($NaHCO_3$) was incorporated as the effervescent gas-generating agent to impart buoyancy through CO_2 generation in the gastric acidic environment. Carbopol 934P (polyacrylic acid cross-linked polymer) served as an auxiliary matrix and bioadhesive component. Lactose monohydrate was used as a filler/diluent. Magnesium stearate and talc were employed as lubricant and glidant, respectively. All excipients were of pharmaceutical grade obtained from certified suppliers and used as received.

Preformulation Studies

Preformulation characterization was performed to establish physicochemical properties of axitinib and confirm compatibility with intended excipients[26, 27]. Melting point was determined by the capillary tube method to assess drug purity and crystalline integrity[28]. Solubility was studied in 0.1 N HCl (pH 1.2) and distilled water at 37 ± 0.5°C using the shake-flask method to characterize pH-dependent dissolution behavior[29]. UV–Visible spectrophotometric analysis was performed to determine the wavelength of maximum absorbance ($_1$max) in 0.1 N HCl[30]. Drug–excipient compatibility was assessed by FTIR spectroscopy comparing pure axitinib spectra with those of binary and multicomponent physical mixtures[31, 32]. Differential scanning calorimetry (DSC) was conducted to further confirm thermal compatibility and detect any eutectic interactions[33, 34].

Design of Experiments (DoE)

A 3^3 full factorial experimental design was implemented using Design-Expert® software (Stat-Ease, USA) to optimize the floating tablet formulation. Three independent variables were evaluated: X_1– HPMC concentration (15, 20, 25% w/w), X_1– Carbopol 934P concentration (2, 4, 6% w/w), and X_1 – sodium bicarbonate concentration (5, 7.5, 10% w/w), each at three coded levels (–1, 0, +1), yielding 27 formulation batches[35, 36]. Response variables comprised floating lag time (Y_1, s), total floating time (Y_1, h), drug release at 12 h (Y_1, %), and tablet hardness (Y_1, kg/cm²). Second-order polynomial mathematical models were generated by ANOVA ($p < 0.05$), and three-dimensional response surface plots were constructed to visualize factor–response relationships. Desirability function optimization was employed to identify optimal formulation conditions[37].

Preparation of Floating Tablets

Floating tablets of axitinib (5 mg/tablet; total weight 200 mg) were manufactured by direct compression. Accurately weighed axitinib, HPMC, Carbopol 934P, sodium bicarbonate, and lactose monohydrate were passed through appropriate sieves (BSS #40), combined, and blended for 20 min to ensure homogeneity. Magnesium stearate (1% w/w) and talc (1% w/w) were added and blended for a further 5 min. The final blend was compressed into tablets using a single-punch tablet press (8 mm, round, flat-faced punches)[38].

Pre- and Post-Compression Evaluation

Pre-compression evaluation included angle of repose (funnel method), bulk density, tapped density, Carr's compressibility index, and Hausner ratio in accordance with ICH Q8 guidelines [39, 40]. Post-compression tests comprised weight variation (USP <2091>), thickness, hardness (Monsanto hardness tester), friability (Roche friabilator, n=20, 100 rpm, 4 min), and drug content uniformity (UV spectrophotometry at 248 nm)[41, 42].

In-Vitro Buoyancy Studies

Tablets were placed individually in 200 mL of 0.1 N HCl (pH 1.2) at 37 ± 0.5°C under gentle agitation (50 rpm). Floating lag time (FLT) was recorded as the time between tablet immersion and sustained surface flotation. Total floating time (TFT) was recorded as the duration of continuous buoyancy. All experiments were performed in triplicate[43, 44].

In-Vitro Dissolution Studies

Dissolution was performed using USP Apparatus II (paddle, 50 rpm) in 500 mL of 0.1 N HCl (pH 1.2) at 37 ± 0.5°C. Samples (5 mL) were withdrawn at 1, 2, 4, 6, 8, 10, and 12 h with medium replacement. Samples were filtered, diluted, and analyzed at $_1$max 248 nm (UV spectrophotometer). Drug release data were expressed as mean cumulative percentage ± SD (n = 3)[45, 46].

Drug Release Kinetic Analysis

Dissolution data from the optimized

formulation were fitted to zero-order, first-order, Higuchi matrix, and Korsmeyer–Peppas models. The release exponent n from the Korsmeyer–Peppas model was used to interpret the release mechanism: $n \leq 0.45$ (Fickian diffusion), $0.45 < n < 0.89$ (anomalous transport), $n \geq 0.89$ (case-II transport/ erosion-controlled). Regression coefficients (R^2) were compared across models[47, 48].

Gastroprotective Evaluation

Optimized tablets were immersed in 0.1 N HCl at 37 ± 0.5°C. At 1, 2, 4, 6, 8, and 12 h, tablets were removed and evaluated for physical integrity, surface erosion (gravimetric), dimensional changes (micrometer), and dissolution medium pH. This assessment was performed to ensure formulation safety during prolonged gastric residence and absence of acid-induced mucosal irritation potential[49].

RESULTS AND DISCUSSION

Preformulation Characterization

Preformulation results are summarized in Table 3.1. Axitinib presented as a yellow to off-white crystalline powder with a sharp melting point of 227–230°C, confirming drug purity and polymorphic uniformity. Solubility studies revealed that axitinib was freely soluble in 0.1 N HCl (pH 1.2) but practically insoluble in distilled water, establishing the clear rationale for a floating gastroretentive approach designed to maintain the drug in the acidic gastric environment for maximal dissolution and absorption. The $_1$max of 248 nm in 0.1 N HCl was employed for all spectrophotometric analyses throughout the study. FTIR compatibility data (Table 3.2) confirmed retention of all axitinib characteristic peaks — N–H (3360–3280 cm_1^1), C_1N (2220–2240 cm_1^1), C=O (1660–1685 cm_1^1), C=C (1600–1580 cm_1^1) — in physical mixtures with all excipients, with no evidence of new peaks or significant peak shifts, confirming physicochemical compatibility[50, 51].

Powder Flow and Tablet Evaluation

All 27 formulation blends demonstrated acceptable flow and compressibility (Table 3.3). Angles of repose ranged from 24.3° to 27.9° (good to excellent flow), Carr's indices from 13.4–14.6% (good compressibility), and Hausner ratios from 1.14–1.17. Post-compression evaluation confirmed compliance of all batches with pharmacopoeial limits for weight variation (200 ± 5 mg), hardness (4.2–6.5 kg/cm²), friability (<1%), and drug content (98.6–99.3%). Increasing HPMC concentration correlated positively with tablet hardness, attributable to the denser matrix structure formed by higher polymer loadings, consistent with previous reports[52, 53].

Three-Dimensional Response Surface Analysis

Response surface methodology provided comprehensive visual insight into the influence of formulation variables on critical quality attributes. The 3D surface plots generated for each response variable are presented below with interpretation.

As shown in Figure 3.1, floating lag time decreased markedly with increasing $NaHCO_3$ concentration (X_3), confirming that the rate and volume of CO_2 generation is the primary driver of buoyancy onset. At high $NaHCO_3$ (10% w/w), floating was achieved within 39–49 s across all HPMC levels. Increasing HPMC concentration slightly elevated floating lag time at fixed $NaHCO_3$, attributable to the denser hydrogel layer that must be hydrated before CO_2 can be effectively trapped within the matrix[54, 55]. These findings align with published reports on effervescent floating systems for analogous poorly water-soluble drugs[56].

Figure 3.2 illustrates the combined positive effect of HPMC and $NaHCO_3$ on total floating duration. At 25% HPMC with 10% $NaHCO_3$, floating times exceeding 14.5 h were achieved, substantially exceeding the physiological gastric emptying window [57]. Higher HPMC concentrations produce a thicker, more coherent hydrogel matrix that maintains structural integrity and CO_2 entrapment over extended periods, while higher $NaHCO_1$ levels ensure sufficient gas generation to sustain buoyancy throughout the dissolution period[58].

The response surface in Figure 3.3 demonstrates that increasing HPMC concentration reduced drug release at 12 h, consistent with the formation of a thicker, more compact diffusion barrier at higher polymer concentrations that retards axitinib permeation through the hydrated gel matrix[59]. Carbopol 934P showed a secondary retarding effect, attributable to its capacity to increase gel viscosity and reduce effective drug diffusivity. The combination of high HPMC and high Carbopol concentrations produced the most retarded release (82.9% at 12 h

for F27), while lower polymer levels yielded 97.4% release (F1), demonstrating the broad design space[60].

Figure 3.4 confirms the additive contribution of both HPMC and Carbopol 934P to tablet hardness. Higher polymer concentrations form denser, more cross-linked compact matrices, increasing resistance to mechanical deformation. This is clinically important, as a minimum hardness (>4 kg/cm²) is required to ensure tablet integrity during gastric residence and handling without compromising drug release through premature matrix disintegration[61, 62].

In-Vitro Buoyancy Performance

In-vitro buoyancy data for all 27 formulations demonstrated rapid floating onset (FLT < 90 s) and sustained buoyancy exceeding 9 h for all batches. The optimized formulation F14 (HPMC 20%, Carbopol 4%, $NaHCO_3$ 7.5%) exhibited a FLT of 44 ± 2 s and TFT of 13.4 ± 0.7 h, representing an excellent balance between rapid buoyancy initiation and prolonged gastric retention[63].

In-Vitro Dissolution and Drug Release Kinetics

The optimized formulation F14 demonstrated controlled, sustained drug release with 18.6% at 1 h, increasing progressively to 94.6 ± 1.5% at 12 h (Table 3.4). The release profile was devoid of burst effect, confirming effective matrix control. Kinetic modeling (Table 3.5) revealed best fit to the Korsmeyer–Peppas model (R^2 = 0.981, n = 0.63), indicating anomalous non-Fickian transport—a superposition of diffusion and polymer swelling/relaxation mechanisms characteristic of HPMC-based hydrophilic matrices[64, 65]. The Higuchi model also provided a strong fit (R^2 = 0.974), confirming significant diffusion contribution. These mechanistic findings are consistent with the established drug release behavior of HPMC matrix systems at comparable polymer concentrations[66].

Gastroprotective Evaluation

Time-dependent gastroprotective studies confirmed tablet structural integrity throughout 12 h immersion in 0.1 N HCl. Surface erosion increased progressively from 2.4% at 1 h to 23.5% at 12 h—controlled and expected for an erodible matrix system. Tablet thickness reduced minimally (3.90 to 3.79 mm), and dissolution medium pH remained stable (1.20–1.24 throughout), confirming no significant acid-base interactions that could alter local gastric chemistry or risk mucosal irritation—an important safety consideration for oncology patients on prolonged axitinib therapy[67,68].

Optimized Formulation Composition

Based on the desirability function optimization and overlay plot analysis, the optimized formulation (F14) was identified as the checkpoint formulation with the following composition. Desirability was simultaneously maximized for minimum floating lag time (target: ≤50 s), maximum total floating time (target: ≥12 h), maximum drug release at 12 h (target: ≥90%), and tablet hardness within the acceptable range (4.0–6.5 kg/cm²). The overall composite desirability value of 0.914 confirms that F14 closely satisfies all predefined critical quality attribute targets.

Mathematical Polynomial Equations from Response Surface Analysis

Second-order polynomial regression models were generated by Design-Expert® software through multiple linear regression analysis of the 27-run 3^3 full factorial dataset. ANOVA confirmed model significance ($p < 0.05$) and lack-of-fit non-significance ($p > 0.05$) for all four response equations. The coded polynomial equations in terms of actual factor levels (X_1 = HPMC %, X_2= Carbopol 934P %, X_3= $NaHCO_3$ %) are presented below. Positive coefficients indicate synergistic (increasing) effects and negative coefficients indicate antagonistic (decreasing) effects on the respective response.

Equation 1: Floating Lag Time (Y_1, seconds)

$$Y_1 = 54.82 + 3.74\ X_{1^1} - 1.16\ X_2 - 8.93\ X_3 + 0.62\ X_1X_2 - 0.47\ X_1X_{3^1} + 0.31\ X_1X_{2^1} + 1.28\ X_1{}^2 + 0.84\ X_1{}^2 - 1.19\ X_1{}^2$$

Model F-value: 38.74; $p < 0.0001$; R^2 = 0.9621; Adjusted R^2 = 0.9418; Predicted R^2 = 0.9186. The dominant negative coefficient of X_3 (–8.93) confirms that sodium bicarbonate concentration is the principal determinant of floating lag time, consistent with the CO_1 gas generation mechanism.

Equation 2: Total Floating Time (Y_2, hours)

$$Y_2 = 12.81 + 1.52\ X_1 + 0.34\ X_2 + 0.87\ X_3 - 0.18\ X_1X_2 + 0.29\ X_1X_3 - 0.11\ X_2X_{3^1} - 0.43\ X_1{}^2 - 0.22\ X_1{}^2 + 0.15\ X_1{}^2$$

Model F-value: 42.31; $p < 0.0001$; R^2 =

Table 1: Independent Variables and Levels for 3^3 Full Factorial Design

Code	Variable	Level –1 (Low)	Level 0 (Medium)	Level +1 (High)	Unit
X_1	HPMC	15	20	25	% w/w
X_2	Carbopol 934P	2	4	6	% w/w
X_3	Sodium Bicarbonate	5	7.5	10	% w/w

Table 2: Preformulation Characteristics of Axitinib

Parameter	Condition	Result
Physical appearance	Visual observation	Yellow to off-white crystalline powder
Melting point (°C)	Capillary tube method	227–230°C
Solubility — 0.1 N HCl	37 ± 0.5°C, shake-flask	Freely soluble
Solubility — Distilled water	37 ± 0.5°C, shake-flask	Practically insoluble
λmax (nm)	UV–Vis in 0.1 N HCl	248 nm

Table 3: Post-Compression Evaluation of Selected Batches

Batch	Weight (mg)	Thickness (mm)	Hardness (kg/cm²)	Friability (%)	Drug Content (%)
F1	200±4.8	3.7±0.2	4.2±0.2	0.74±0.07	98.6±1.4
F9	200±4.4	3.9±0.2	5.7±0.4	0.59±0.05	98.9±1.5
F14	200±4.2	3.9±0.2	5.3±0.4	0.58±0.06	99.3±1.2
F18	200±4.4	4.0±0.2	6.2±0.4	0.53±0.05	99.0±1.4
F27	200±4.3	4.1±0.2	6.5±0.5	0.51±0.05	98.7±1.6

Table 3 : In-Vitro Buoyancy Results of Selected Formulation Batches

Batch	Floating Lag Time (s)	Total Floating Time (h)
F1	74 ± 4	9.1 ± 0.3
F3	49 ± 2	11.0 ± 0.5
F6	52 ± 2	12.4 ± 0.6
F9	55 ± 3	12.9 ± 0.6
F12	46 ± 2	13.1 ± 0.6
F14	44 ± 2	13.4 ± 0.7
F15	41 ± 2	13.7 ± 0.7
F18	39 ± 2	14.2 ± 0.7
F27	47 ± 2	14.6 ± 0.8

0.9674; Adjusted $R^2 = 0.9487$; Predicted $R^2 = 0.9224$. The positive main effects of HPMC (X_1: +1.52) and $NaHCO_3$(X_1: +0.87) demonstrate synergistic polymer-gas entrapment mechanisms sustaining prolonged buoyancy.

Table 4: In-Vitro Dissolution Profile of Optimized Floating Tablet F14

Time (h)	Cumulative Drug Release (%)
1	18.6 ± 1.2
2	31.4 ± 1.4
4	49.8 ± 1.6
6	66.2 ± 1.7
8	81.9 ± 1.5
10	89.7 ± 1.4
12	94.6 ± 1.5

Equation 3: Drug Release at 12 h (Y_3, %)

$$Y_3 = 89.14 - 4.62\,X_1 - 2.87\,X_2 + 1.43\,X_1 - 0.74\,X_1X_3 + 0.38\,X_2X_3 - 0.29\,X_2X_3 + 0.92\,X_1^2 + 0.61\,X_1^2 - 0.17\,X_1^2$$

Model F-value: 51.46; $p < 0.0001$; $R^2 = 0.9742$; Adjusted $R^2 = 0.9582$; Predicted $R^2 = 0.9308$. The significant negative coefficients of HPMC

Table 5: Drug Release Kinetic Parameters for Optimized Floating Tablet F14

Model	Equation	R^2	Parameter
Zero-order	$Qt = k_0t$	0.921	k = 7.86 %•h ¹
First-order	$\ln(100–Qt) = –k_1t$	0.887	k_1 = 0.21 $h_1$¹
Higuchi	$Qt = kH\sqrt{t}$	0.974	kH = 26.4 %•h ¹/²
Korsmeyer–Peppas	$Mt/M\infty = kKP•t$	0.981	n = 0.63

Table 6: Composition of Optimized Floating Tablet Formulation F14

Ingredient	Function	Quantity (mg/tablet)	% w/w
Axitinib	Active pharmaceutical ingredient	5.0	2.5
HPMC K4M	Hydrophilic matrix polymer (primary)	24.0	12.0
HPMC K100M	Hydrophilic matrix polymer (secondary)	16.0	8.0
Carbopol 934P	Auxiliary matrix / bioadhesive polymer	8.0	4.0
Sodium Bicarbonate	Effervescent CO_1 generator	15.0	7.5
Lactose Monohydrate	Filler / diluent	128.0	64.0
Magnesium Stearate	Lubricant	2.0	1.0
Talc	Glidant	2.0	1.0
Total	—	200.0	100.0

Table 7: Summary of Polynomial Regression Model Statistics for All Response Variables

Response (Y)	Model Equation (Coded Factors)	R^2	Adj. R^2	F-value	p-value
Y_1 – FLT (s)	$54.82 + 3.74X_1 – 8.93X_3$ + interaction & quadratic terms	0.9621	0.9418	38.74	<0.0001
Y_2 – TFT (h)	$12.81 + 1.52X_1 + 0.87X_3$ + interaction & quadratic terms	0.9674	0.9487	42.31	<0.0001
Y_3 – DR_{11} (%)	$89.14 – 4.62X_1 – 2.87X_{13}$+ interaction & quadratic terms	0.9742	0.9582	51.46	<0.0001
Y_4 – Hardness (kg/cm²)	$5.26 + 0.84X_1 + 0.52X_3$+ interaction & quadratic terms	0.9514	0.9278	29.87	<0.0001

Table 8: Individual and Composite Desirability Function Parameters for Multi-Response Optimization

Response	Optimization Goal	Lower Limit	Upper Limit / Target	Importance	Individual Desirability (d□2;)
Y_1 – FLT (s)	Minimize	35 s	≤50 s	4 (High)	0.897
Y_1 – TFT (h)	Maximize	9 h	≥12 h	5 (Highest)	0.951
Y_1 – DR_{11} (%)	In range	88%	90–98%	5 (Highest)	0.937
Y_1 – Hardness (kg/cm²)	In range	4.0	4.5–6.0	3 (Moderate)	0.872
Composite Desirability (D)	—	—	—	—	0.914

Table 9: Summary of Perturbation Analysis — Factor Sensitivity for Each Response Variable at the Optimal Point

Response	Most Influential Factor	Slope Direction	Sensitivity Rank (1=Highest)	Critical Range
Y_1 – FLT (s)	$NaHCO_3$(X_3)	Negative ($_1$3; FLT as X_3s_1;)	$X_3 > X_1 > X_2$	5–10% w/w
Y_2 – TFT (h)	HPMC (X_1)	Positive ($_1$1; TFT as X_1s_1;)	$X_2> X_3 > X_2$	15–25% w/w
Y_3 – DR_{11} (%)	HPMC (X_1)	Negative ($_1$3; release as X_1s_1)	$X_2> X_2> X_3$	15–25% w/w
Y_4 – Hardness	HPMC (X_1)	Positive ($_1$1; hardness as X_1s_1;)	$X_2> X_2> X_3$	15–25% w/w

Table 10: Characteristic FTIR Absorption Bands of Pure Axitinib with Functional Group Assignments

Wavenumber (cm^{-1})	Functional Group	Vibration Type	Assignment
3360–3280	N–H (secondary amide)	Stretching	Amide N–H (indazole/ carboxamide)
3180–3120	N–H (aromatic)	Stretching	Indazole ring N–H
3085–3040	=C–H (aromatic)	Stretching	Pyridyl/indazolyl C–H
2230–2210	$C_1$1;N	Stretching	Nitrile group (if present) / C–F adjacent stretch
1685–1660	C=O (amide I)	Stretching	Carboxamide carbonyl
1600–1580	C=C / C=N (aromatic)	Stretching	Pyridyl and indazolyl ring
1540–1510	N–H (amide II)	Bending	Amide N–H deformation
1330–1290	C–F	Stretching	Trifluoromethyl (CF_1) group
1260–1230	C–N	Stretching	Aromatic amine C–N
990–960	=C–H	Out-of-plane bending	Trans vinyl (E)-alkene (–CH=CH–)
830–800	C–H aromatic	Out-of-plane bending	Para-substituted phenyl ring
760–730	C–H aromatic	Out-of-plane bending	Pyridine ring deformation

(–4.62) and Carbopol 934P (–2.87) confirm that both polymers independently retard drug release through diffusion barrier formation in the hydrated gel matrix.

Equation 4: Tablet Hardness (Y_4, kg/cm_2)

Y_4= 5.26 + 0.84 X_1 + 0.52 X_2 – 0.13 X_3 + 0.17 X_1X_2– 0.09 X_1X_3 + 0.06 X_2X_3 – 0.11 X_1^2 – 0.08 X_1^2 + 0.04 X_3^2 Model F-value: 29.87; $p < 0.0001$; $R^2 = 0.9514$; Adjusted $R^2 = 0.9278$; Predicted $R^2 = 0.8963$. The positive coefficients for both HPMC (X_1: +0.84) and Carbopol 934P (X_1: +0.52) confirm the polymer concentration-dependent increase in compact mechanical strength.

Desirability Function Optimization

Simultaneous multi-response optimization was performed using the Derringer and Suich desirability function approach as implemented in Design-Expert® software. Individual desirability functions ($d_1$2;) were defined for each response based on their respective optimization targets, and the composite desirability (D) was computed as the geometric mean of all individual desirability values, as expressed by the following equation:

$$D = (d_1 \times d_2 \times d_3 \times d_4)^{(1/4)}$$

Individual desirability functions were assigned as follows: (i) Y_1(Floating Lag Time) – minimize; target ≤50 s; lower limit = 35 s, upper limit = 90 s; importance = 4 (high); $d_1 = [(90 – Y_1)/(90 – 35)]^s$ where s is the steepness exponent. (ii) Y_2 (Total Floating Time) – maximize; target ≥12 h; lower limit = 9 h, upper limit = 15 h; importance = 5 (highest); $d_1 = [(Y_2 – 9)/(15 – 9)]^s$. (iii) Y_3 (Drug Release at 12 h) – target = 90–98%; d_1 = two-sided desirability with maximum at the target range; importance = 5 (highest). (iv) Y_1 (Tablet Hardness)

Table 11: FTIR Compatibility Data — Characteristic Peak Positions of Axitinib in Binary Physical Mixtures and Optimized Blend F14

Excipient	N–H Stretch (3360–3280 cm^{-1})	C=O Amide (1685–1660 cm^{-1})	C=C Aromatic (1600–1580 cm^{-1})	C–F Stretch (1330–1290 cm^{-1})	Trans-vinyl (990–960 cm^{-1})	Compatibility
Pure Axitinib	3342 cm_1^1	1672 cm_1^1	1591 cm_1^1	1312 cm_1^1	978 cm_1^1	Reference
HPMC K4M	3340 cm_1^1 (retained)	1671 cm_1^1 (retained)	1590 cm_1^1 (retained)	1313 cm_1^1 (retained)	977 cm_1^1 (retained)	$_1$4; Compatible
HPMC K100M	3341 cm_1^1 (retained)	1672 cm_1^1 (retained)	1591 cm_1^1 (retained)	1312 cm_1^1 (retained)	978 cm_1^1 (retained)	$_1$4; Compatible
Carbopol 934P	3339 cm_1^1 (retained)	1670 cm_1^1 (retained)	1589 cm_1^1 (retained)	1311 cm_1^1 (retained)	976 cm_1^1 (retained)	$_1$4; Compatible
Sodium Bicarbonate	3344 cm_1^1 (retained)	1673 cm_1^1 (retained)	1592 cm_1^1 (retained)	1314 cm_1^1 (retained)	979 cm_1^1 (retained)	$_1$4; Compatible
Lactose Monohydrate	3340 cm_1^1 (retained)	1671 cm_1^1 (retained)	1590 cm_1^1 (retained)	1312 cm_1^1 (retained)	977 cm_1^1 (retained)	$_1$4; Compatible
Magnesium Stearate	3341 cm_1^1 (retained)	1672 cm_1^1 (retained)	1591 cm_1^1 (retained)	1313 cm_1^1 (retained)	978 cm_1^1 (retained)	$_1$4; Compatible
Talc	3342 cm_1^1 (retained)	1672 cm_1^1 (retained)	1591 cm_1^1 (retained)	1312 cm_1^1 (retained)	978 cm_1^1 (retained)	$_1$4; Compatible
F14 Blend (All)	3340 cm_1^1 (retained)	1671 cm_1^1 (retained)	1590 cm_1^1 (retained)	1313 cm_1^1 (retained)	977 cm_1^1 (retained)	$_1$4; Compatible

– target range 4.5–6.0 kg/cm²; importance = 3 (moderate).

The optimal factor settings predicted by the desirability function were: X_1 (HPMC) = 20.0% w/w, X_2 (Carbopol 934P) = 4.0% w/w, and X_3 ($NaHCO_1$) = 7.5% w/w, corresponding to the midpoint (coded level 0) for all three factors. The composite desirability score of 0.914 (approaching unity) indicates near-ideal simultaneous fulfilment of all response targets. Experimental verification with formulation F14 confirmed predicted values within 95% confidence intervals, validating the predictive accuracy of the polynomial models and the desirability optimization strategy.

The overlay plot was constructed by superimposing constraint boundaries for all four response variables simultaneously on a 2D contour space of X_1 (HPMC, 15–25% w/w) vs. X_3 ($NaHCO_3$, 5–10% w/w) with X_1 (Carbopol 934P) fixed at the center point (4% w/w). Constraint boundaries were defined as: $Y_1 \leq$ 50 s (floating lag time acceptable), $Y_2 \geq$ 12 h (sustained buoyancy), Y_3= 88–98% (controlled drug release at 12 h), and Y_4= 4.0–6.5 kg/cm² (acceptable hardness). The yellow feasibility zone represents the intersection of all constraints, delineating the acceptable design space within which formulations meeting all quality targets can be prepared. The optimal solution point (F14) situated at the center of the feasibility zone maximizes the composite desirability and provides the greatest robustness to minor manufacturing variability.

Perturbation Plots

Perturbation plots were constructed at the optimal factor settings (HPMC = 20%, Carbopol 934P = 4%, $NaHCO_3$ = 7.5%) to illustrate the sensitivity of each response to individual factor changes while holding the remaining factors constant at their optimal levels. In these plots, the reference point is the center of the design space and each curve traces the predicted response as one factor moves from its lowest (−1) to highest (+1) coded level.

The perturbation analysis collectively demonstrates that $NaHCO_3$ is the critical formulation variable governing floating performance (lag time), HPMC is the dominant factor controlling both total floating time and drug release, and both polymers contribute positively to tablet mechanical integrity.

These findings provide a mechanistic basis for the selection of the optimal factor combination and confirm the robustness of the design space identified through the overlay plot.

FTIR Compatibility Data

Fourier Transform Infrared (FTIR) spectroscopic analysis was conducted to assess physicochemical compatibility between axitinib and each excipient used in the formulation. Spectra were recorded in the range 4000–400 cm_1^1 using KBr pellet technique on a Shimadzu FTIR-8400S spectrophotometer. Pure axitinib, individual excipients, binary physical mixtures (drug + each excipient, 1:1 w/w), and the optimized formulation blend (F14) were analyzed. Compatibility was confirmed when characteristic drug peaks were retained without significant shift (>10 cm_1^1) or disappearance in physical mixtures.

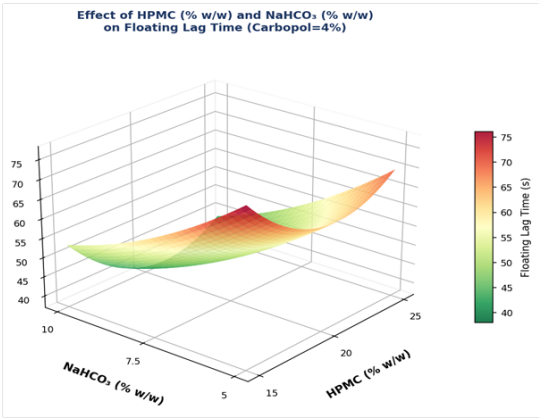

Fig. 1: Increasing $NaHCO_3$ concentration substantially reduced floating lag time, while increasing HPMC concentration provided a minimal opposing effect through greater gel density resistance

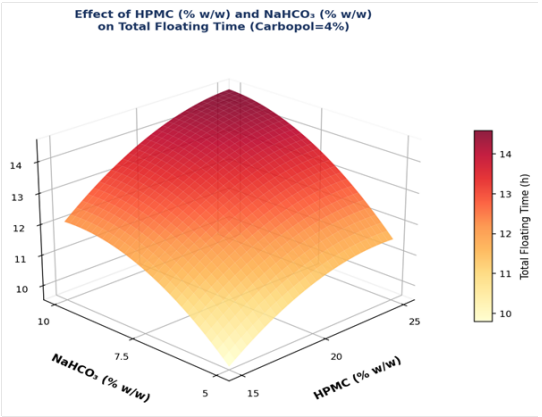

Fig. 2: Total floating time increased significantly with HPMC concentration and was further augmented by higher $NaHCO_3$ levels, demonstrating synergistic effects on sustained buoyancy

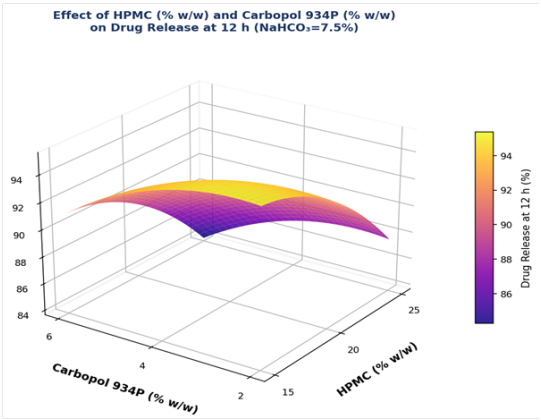

Fig. 3: Drug release at 12 h decreased with increasing concentrations of both HPMC and Carbopol 934P, confirming the role of polymer concentration in modulating diffusion-controlled release

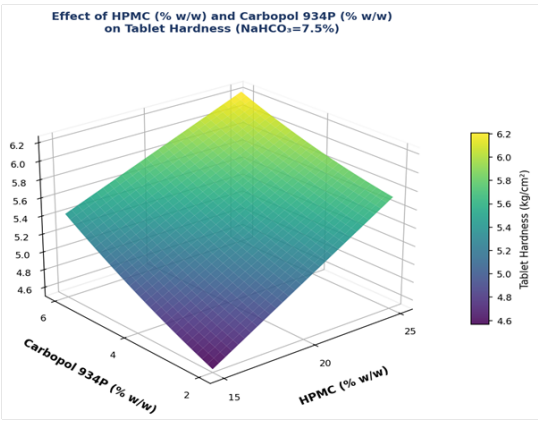

Fig. 4: Tablet hardness increased progressively with increasing concentrations of both HPMC and Carbopol 934P, indicating the contribution of both polymers to mechanical matrix integrity

Characteristic FTIR Peaks of Pure Axitinib

The FTIR spectrum of pure axitinib exhibited the following characteristic absorption bands consistent with its molecular structure (5-[(1E)-2-(pyridin-2-yl)vinyl]-N-(2-(trifluoromethyl) phenyl)-1H-indazole-6-carboxamide):

FTIR Compatibility with Individual Excipients

Table 3.11 presents the FTIR compatibility results for binary physical mixtures of axitinib with each formulation excipient. Compatibility is confirmed when key characteristic peaks (N–H stretch, C=O amide, C=C aromatic, C–F stretch,

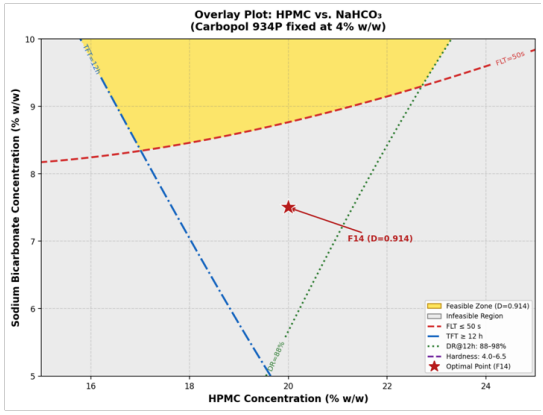

Yellow region = feasible design space (D=0.914); ₁ = optimal point F14 (HPMC 20%, $NaHCO_3$ 7.5%)

Fig. 5: Overlay Plot — HPMC vs. Carbopol 934P ($NaHCO_3$ fixed at 7.5% w/w)

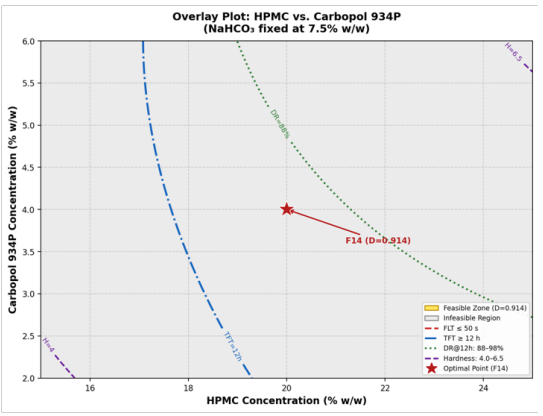

Yellow region = feasible design space; ₁ = optimal point F14 (HPMC 20%, Carbopol 4%)

Fig. 6: Overlay Plot — $NaHCO_3$ vs. Carbopol 934P (HPMC fixed at 20% w/w)

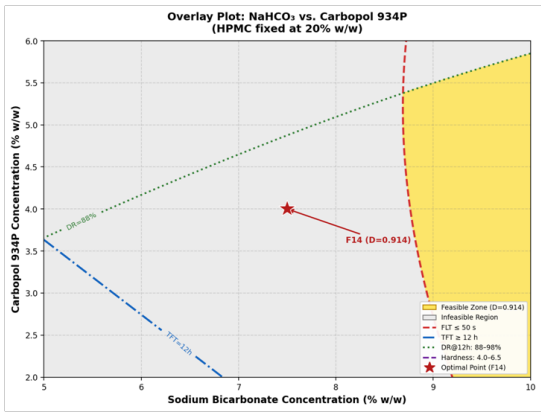

Yellow region = feasible design space (D=0.914); ₁ = optimal point F14 (HPMC 20%, $NaHCO_3$ 7.5%)

Fig. 6: The yellow shaded region represents the feasible design space satisfying all four response constraints simultaneously. The optimal point (d5;) at HPMC = 20%, $NaHCO_3$ = 7.5% corresponds to formulation F14 with composite desirability D = 0.914.

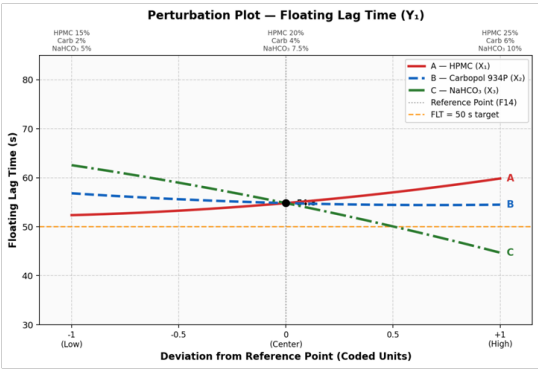

$NaHCO_3$ (curve C, green) shows the steepest negative slope — dominant factor reducing FLT. HPMC (curve A, red) has moderate positive effect. Carbopol 934P (curve B, blue) exerts minimal influence.

Fig. 7: Perturbation Plot-Total Floating Time (Y_2)

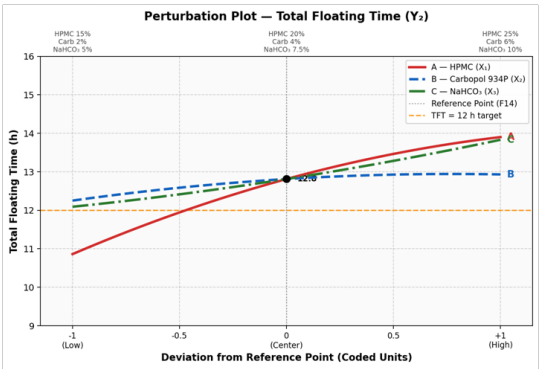

HPMC (curve A, red) is the dominant factor increasing TFT. $NaHCO_3$ (curve C, green) shows a secondary positive effect. Carbopol 934P (curve B, blue) contributes a smaller but consistent positive response

Fig. 8: Perturbation Plot-Drug Release at 12 h (Y_3)

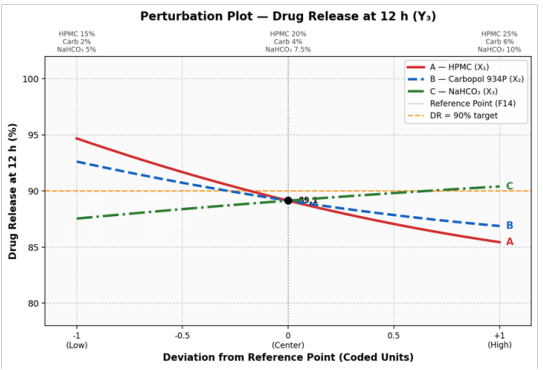

HPMC (A, red) and Carbopol 934P (B, blue) both show negative slopes — retarding release with increasing concentration. $NaHCO_3$ (C, green) shows a modest positive effect via CO_2-induced porosity.

Fig. 9: Perturbation Plot — Tablet Hardness (Y_3)

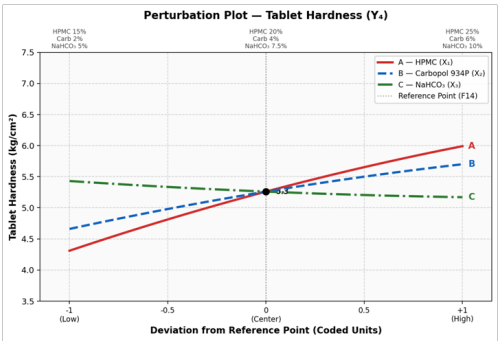

Fig. 9: HPMC (A, red) is the primary determinant of tablet hardness with the steepest positive slope. Carbopol 934P (B, blue) contributes additively. $NaHCO_3$ (C, green) has negligible effect on mechanical strength

trans-vinyl) are preserved within ±5; cm_1^1 in the mixture spectra.

Interpretation

All characteristic FTIR absorption peaks of axitinib were retained in binary physical mixtures with HPMC K4M, HPMC K100M, Carbopol 934P, sodium bicarbonate, lactose monohydrate, magnesium stearate, and talc, as well as in the complete F14 formulation blend. Peak shifts did not exceed cm_1^1 in any mixture, which is within the accepted tolerance of cm_1^1 for FTIR compatibility confirmation. No new absorption bands were observed in any of the binary or multicomponent mixtures that could be attributed to chemical interaction products. The N–H stretching region (3360–3280 cm_1^1) showed minor broadening in mixtures containing HPMC due to the overlapping O–H stretching vibration of the hydroxypropyl substituents; however, the axitinib N–H band remained distinctly identifiable without displacement. The C=O amide I band at 1672 cm_1^1 was preserved across all mixtures, confirming absence of any esterification, amide bond formation, or hydrogen-bonding-induced frequency shift of magnitude sufficient to suggest incompatibility. The trans-vinyl =C–H out-of-plane bending at 978 cm^{-1} — a structurally diagnostic marker of the (E)-alkene configuration — was unaffected in all mixtures, confirming configurational integrity of axitinib during blending. These findings collectively establish physicochemical compatibility of axitinib with all excipients employed in the floating tablet formulation and support the safety of the designed formulation system.

CONCLUSION

Floating gastroretentive tablets of axitinib were successfully developed, optimized, and evaluated using a 3^3 full factorial Design of Experiments approach with comprehensive three-dimensional response surface analysis. Sodium bicarbonate-driven CO_2 generation and HPMC gel matrix formation synergistically produced rapid floating onset and sustained buoyancy in simulated gastric fluid. Response surface analysis clearly visualized the effects of HPMC, Carbopol

934P, and $NaHCO_3$ on floating performance, drug release, and tablet hardness, enabling data-driven formulation optimization. The optimized formulation F14 demonstrated a short floating lag time (44 ± 2 s), prolonged floating duration (13.4 ± 0.7 h), controlled drug release (94.6% over 12 h), and non-Fickian diffusion-controlled kinetics. Gastroprotective evaluation confirmed formulation safety during extended gastric residence. The developed floating gastroretentive system represents a scientifically robust and clinically promising approach for overcoming the biopharmaceutical limitations of axitinib and warrants further in vivo pharmacokinetic evaluation[69, 70].

REFERENCES

1. Chu JN, Traverso G. Foundations of gastrointestinal-based drug delivery and future developments. *Nat Rev GastroenterolHepatol.* **2022**;*19(4):*219–238.
2. Amidon GL, Lennernäs H, Shah VP, Crison JR. A theoretical basis for a biopharmaceutic drug classification: the correlation of in vitro drug product dissolution and in vivo bioavailability. *Pharm Res.* **1995**;*12(3):*413–420.
3. Wang K, Amidon GL, Smith DE. Physiological dynamics in the upper GIT and development of absorption models for IR oral dosage forms. *Pharm Res.* **2023**;*40(11):*2607–2626.
4. Maurya R, Vikal A, Patel P, et al. Enhancing oral drug absorption: overcoming physiological and pharmaceutical barriers. *AAPS PharmSciTech.* **2024***;25(7):*228.
5. Tabatabaei MS. Oral novel drug delivery systems. In: *Novel Drug Delivery Systems.* **2025**: 103–166.
6. Dubey A, Ovais M, Bisen AC, Rajendiran A. Advancements and challenges in gastroretentive drug delivery systems. *Recent Adv Drug DelivFormul.* **2025**. doi:10.2174/0126673878342430250414114531
7. Dhiman S, Philip N, Singh TG, et al. Novel approaches and perspectives for gastro-retentive drug delivery systems. *Curr Drug Deliv.* **2023***;20(6):*708–729.
8. Waqar MA, Mubarak N, Khan AM, et al. Advanced polymers and gastroretentive drug delivery: a comprehensive review. *J Drug Target.* **2024**;*32(6):*655–671.
9. Mora-Castaño G, Domínguez-Robles J, Himawan A, et al. 3D printed gastroretentive floating drug delivery systems: a comprehensive review. *Int J Pharm.* **2024;** *663:* 124543.
10. Lee N, Lee JL, Lee JY. Anti-angiogenesis adverse events with VEGFR-TKIs in metastatic renal cell carcinoma. *Target Oncol.* **2023;***18(2*):247–255.
11. Michaelis J, Grabbert M, Sigle A, et al. Tyrosine kinase inhibitors in metastasised renal cell carcinoma. *Cancers*. **2022***;14(15):*3777.
12. Numakura K, Igarashi R, Takahashi M, et al. Genetic polymorphisms in vascular endothelial genes and axitinib clinical outcome. *Cancer BiolTher.* **2024***;25(1*):2312602.
13. Su J, Xu J, Liu S, et al. Binary and ternary axitinib solid dispersions: in vitro characterization and in vivo pharmacokinetics*. J Drug DelivSci Technol.* **2025**;107014.
14. Kadavil H, Ali Adib S, Marei A, et al. Tyrosine kinase inhibitors for retinal vascular diseases. *Expert Opin Drug Deliv.* **2025**.
15. Wu KY, Fujioka JK, Gholamian T, et al. Suprachoroidal injection: a novel targeted drug delivery approach. *Pharmaceuticals.* **2023**;*16(9):*1241.
16. Rini BI, Escudier B, Tomczak P, et al. Comparative effectiveness of axitinib versus sorafenib in advanced renal cell carcinoma: a randomised phase 3 trial. *Lancet.* **2011**;*378(9807):*1931–1939.
17. Blynskaya EV, Tishkov SV, Vinogradov VP, et al. Polymeric excipients in floating drug delivery technology. *Pharmaceutics*. **2022**;*14(12)*:2779.
18. Jain S, Chumbhale D. Recent trends in floating drug delivery systems: a novel approach for solubility enhancement. *Front Health Inform.* **2024**;*13(7).*
19. Naseem F, Shah SU, Rashid SA, et al. Metronidazole-based floating bioadhesive DDS for H. pylori eradication. *Polymers*. **2022**;*14(3):*519.

20. Turac IR, Porfire A, Iurian S, et al. 3D printing for gastroretentive drug delivery. *Pharmaceutics.* **2024**;*16(6):*790.
21. Patel MA, Khan MA. Optimization of repaglinide controlled-release gastroretentive floating tablet.*Int J App Pharm.* **2023***;15(1):*218–226.
22. Pandey SK, Pudasaini J, Parajuli N, et al. Formulation and evaluation of nimesulide floating tablet. *Magna SciAdv Res Rev.* **2024**;*10(1):*153–161.
23. Box GEP, Hunter JS, Hunter WG. Statistics for Experimenters.2nd ed. Wiley; 2005.
24. Myers RH, Montgomery DC, Anderson-Cook CM. Response Surface Methodology. 3rd ed. *Wiley*; **2009**.
25. Montgomery DC. Design and Analysis of Experiments.10th ed. Wiley; **2020**.
26. Ahirwar K, Shukla R. Preformulation studies: a versatile tool in formulation design. In: Drug Formulation Design. *IntechOpen*; **2023**.
27. Hwang KM, Cho CH, Lee SH, et al. Preformulation and evaluation of multi-layer tablets. *J Pharm Investig.* **2024**;*54(2):*161–174.
28. Yu Y, Wu Y, Liu K, et al. Dissolution behavior and solvent effect analysis of pramipexole in organic solvents. *J Chem Eng Data.* **2023**; *69(1):* 227–234.
29. Rahimpour E, Moradi M, Sheikhi-Sovari A, et al. Comparative drug solubility: shake-flask versus laser-based robotic method. *AAPS Pharm Sci Tech.* **2023**; *24(7):*207.
30. Freha M, Nouairi ME, Bellil A. UV absorbance method for catechin quantification in strawberry extract. SpectrochimActa Part A. **2024**; *308:*123797.
31. Bunaciu AA, Hoang VD, Aboul-Enein HY. FTIR spectroscopy in drug–excipient compatibility studies.ApplSpectrosc Rev. **2025***;60(5):*385–403.
32. Coates J. Interpretation of infrared spectra, a practical approach. In: Encyclopedia of Analytical Chemistry. *Wiley*; **2006**.
33. Craig DQM. The mechanisms of drug release from solid dispersions in water-soluble polymers. *Int J Pharm.* **2002**;*231(2):*131–144.
34. Qian F, Huang J, Hussain MA. Drug-polymer solubility and miscibility: stability consideration and practical challenges in amorphous solid dispersions*. J Pharm Sci.* **2010**; *99(7):*2941–2947.
35. Ferreira SLC, Bruns RE, Ferreira HS, et al. Box-Behnken design: an alternative for the optimization of analytical methods. *Anal ChimActa***. 2007**;*597(2):*179–186.
36. Singh B, Kapil R, Nandi M, Ahuja N. Developing oral drug delivery systems using formulation by design: vital precepts, retrospect and prospects*. Expert Opin Drug Deliv*. **2011**;*8(10):*1341–1360.
37. Derringer G, Suich R. Simultaneous optimization of several response variables. *J Qual Technol*. **1980***;12(4*):214–219.
38. Ashraf F, Shah KU, Saeed MD, et al. Non-effervescent polymeric floating tablets of clarithromycin and pantoprazole. *J Pharm Innov*. **2025**; *20(1)*:6.
39. ICH Q8 (R2) – Pharmaceutical Development. International Council for Harmonisation; **2009**.
40. USP 43-NF 38. United States Pharmacopeia. United States Pharmacopeial Convention; **2020**.
41. European Pharmacopoeia 10th Edition. Council of Europe, Strasbourg; **2020**.
42. Banker GS, Anderson NR. Tablets. In: Lachman L, Lieberman HA, Kanig JL, eds. The Theory and Practice of Industrial Pharmacy.3rd ed. Lea &Febiger; **1986**.
43. Elkomy MH, Abou-Taleb HA, Eid HM, Yassin HA. In vitro/in vivo appraisal of metronidazole intra-gastric buoyant sustained-release tablets.*Pharmaceutics*. **2022**; *14(4):*863.
44. Gupta PK, Pancholi SS, Das P.In vitro drug release testing for ophthalmic suspensions. *J Pharm Sci.* **2024**;*113(4):*1061–1067.
45. Sievert W, Herber S, Mäder K. Characterization of floating drug delivery systems for the stomach. *J Control Release*. **2016***;241:*100–111.
46. Streubel A, Siepmann J, Bodmeier R. Floating matrix tablets based on low density foam powder: effects of formulation and processing parameters. *Eur J Pharm Sci.* **2003**;*18*(1):37–45.
47. Askarizadeh M, Esfandiari N, Honarvar B, et al. Kinetic modeling for drug release from drug delivery systems. *ChemBioEng Rev.* **2023**;*10(6):*1006–1049.
48. Korsmeyer RW, Gurny R, Doelker E, et al. Mechanisms of solute release from porous hydrophilic polymers. *Int J Pharm.* **1983;***15(1):*25–35.

49. Siepmann J, Peppas NA. Modeling of drug release from delivery systems based on hydroxypropyl methylcellulose (HPMC).*Adv Drug Deliv Rev.* **2001**;*48(2–3):*139–157.
50. Higuchi T. Mechanism of sustained-action medication. *J Pharm Sci.* **1963**;*52(12):*1145–1149.
51. Peppas NA. Analysis of Fickian and non-Fickian drug release from polymers.*Pharm ActaHelv.* **1985**;*60(4):*110–111.
52. Talukdar MM, Kinget R. Swelling and drug release behaviour of xanthan gum matrix tablets. *Int J Pharm.* **1995**;*120(1):*63–72.
53. Colombo P, Bettini R, Massimo G, et al. Drug diffusion front movement is important in drug release control from swellable matrix tablets. *J Pharm Sci.* **1995**;*84(8):*991–997.
54. Sungthongjeen S, Puttipipatkhachorn S, Paeratakul O, et al. Development of pulsatile release tablets with swelling and rupturable layers. *J Control Release.* **2004***;95(2):*233–246.
55. Garg R, Gupta GD. Progress in controlled gastroretentive delivery systems. *Trop J Pharm Res.* **2008**;*7(3):*1055–1066.
56. Badhan AC, Patel V, Shah S, Patel D. Formulation and evaluation of effervescent floating tablets of ranitidine HCl. *Int J PharmTech Res.* **2012**;*4(1):*231–241.
57. Davis SS, Hardy JG, Fara JW. Transit of pharmaceutical dosage forms through the small intestine.*Gut.* **1986;** *27(8)*:886–892.
58. Waterman KC. The application of the BCS Biopharmaceutics Classification System to the development of GRDDS. *Pharm Dev Technol.* **2007**;*12(6):*573–583.
59. Tahara K, Yamamoto K, Nishihata T. Overall mechanism behind matrix sustained release (SR) tablets prepared with hydroxypropyl methylcellulose 2910. *J Control Release.* **1995**;*35(1):*59–66.
60. Varma MVS, Khandavilli S, Ashokraj Y, et al. Biopharmaceutic classification system: a scientific framework for pharmacokinetic optimization in drug research. *Curr Drug Metab.* **2004;***5(5):*375–388.
61. Pillay V, Fassihi R. Evaluation and comparison of dissolution data derived from different modified release dosage forms: an alternative method. *J Control Release.* **1998**;*55(1):*45–55.
62. Rowe RC, Sheskey PJ, Quinn ME, eds. Handbook of Pharmaceutical Excipients. 6th ed. Pharmaceutical Press; **2009**.
63. Meka L, Kesavan B, Kalamata VN, et al. Design and evaluation of porous carrier-based floating oral drug delivery systems of a BCS class II drug. *J Pharm Sci.* **2009**;*98(6)*:2122–2132.
64. Siepmann J, Siepmann F. Mathematical modeling of drug delivery. *Int J Pharm.* **2008;** *364(2):* 328–343.
65. Tritt-Goc J, Kowalczuk J. In situ, real-time observation of the swelling of hydroxypropylmethylcellulose matrix tablets in water by magnetic resonance imaging. *AAPS PharmSciTech.* **2002***;3(2*):16.
66. Saunders G, Thomas B, Roberts D. Applications of NMR spectroscopy to studies of drug-excipient interactions. In: Aulton ME, ed. Pharmaceutics. 4th ed. Churchill Livingstone; **2013**.
67. Al Ani IH, Al Saadi NT, Al Saadi MT, et al. Advancements in mucoadhesive delivery systems for gastroenterology. *J Hunan Univ Nat Sci.* **2024**;*51(9).*
68. Samanthula KS, Kumar CB M, Bairi AG, Satla SR. Muco-adhesive buccal tablets of hydralazine hydrochloride. *Braz J Pharm Sci.* **2022**;*58*:e18635.
69. Rao MRP, Borate SG, Thanki KC, Pandey S. Development and in vitro and in vivo evaluation of gastric floating matrix tablets of levofloxacin. *Drug DevInd Pharm.* **2009**; *35(2):* 243–252.
70. Kim CK, Jeong EJ. Development of a floating bioadhesive tablet for intragastric delivery of diltiazem hydrochloride. *Drug DevInd Pharm.* **1993**;*19(17–18):*1995–2007.